

EFFECT OF VIBRATION AND GAS VELOCITY ON U_{MF} AND ELUTRIATION RATE CONSTANT OF STARCH POWDERS

Siti Masrinda Tasirin^{1*} and Nornizar Anuar²

¹Department of Chemical and Process Engineering
Universiti Kebangsaan Malaysia
43600 Bangi, Malaysia.

²Faculty of Mechanical Engineering
Universiti Teknologi MARA
Shah Alam, Malaysia.

(masrinda@vlsi.eng.ukm.my)

RINGKASAN: *Kajian sekumpul ke atas hidrodinamik proses pembendaliran dan fenomena pengirangan zarah kanji yang tergolong di dalam kumpulan zarah C telah dilakukan. Menggunakan sebuah turus terbendalir bergetar, dapat dianggarkan bahawa saiz purata zarah efektif, d_{agg} pada halaju pembendaliran minimum, U_{mf} adalah 2 atau 3 kali ganda lebih besar dari saiz purata zarah suapan. Pembentukan aglomerat di dalam lapisan telah mengurangkan kehilangan zarah atau bahan oleh fenomena pengirangan. Telah diperolehi bahawa untuk kesemua zarah kajian, pengirangan hanyalah di dalam julat 0.5-1.7 % daripada jumlah zarah halus sebenar yang sepatutnya teriring keluar daripada turus lapisan terbendalir. Nilai pemalar kadar pengirangan bagi zarah didapati berkurang dengan pertambahan saiz zarah. Menggunakan kriteria dari Ma dan Kato (1998), telah diperolehi bahawa nombor kejelekitan kritikal, N_{coh}^* adalah bernilai 19.*

ABSTRACT: Batch experimental work on fluidisation hydrodynamic and entrainment phenomena of Group C starch powders was studied. Using a vibrated fluidised bed, it was estimated that the effective mean particle size, d_{agg} , in the bed at minimum fluidisation velocity, U_{mf} , was 2 or 3 times larger than the actual mean particle size of each feed material. The formation of agglomerates in the bed has reduced material loss by entrainment. It was found that for all the powder used, entrainment was only in the range of 0.5-1.7% of the total fines that should be entrained from the bed. The elutriation rate constants of the powders decreased as particle size decreased. By adapting the criterion proposed by Ma and Kato (1998), it was found in this case that the critical cohesion number, N_{coh}^* is 19.

KEYWORDS: Fluidisation, group C, vibration, entrainment, elutriation rate constant

INTRODUCTION

Following the rapid growth of applications of ultra-fine particles in industry, fluidisation of fine particles has become an emerging field. Generally, these sub-micron particles are classified as group C powders (Geldart, 1973), which are adhesive and hard to fluidise. In general, there are two methods to improve the fluidisation quality of fine particles. One is by external forces, such as vibration and, magnetic field (Mori *et al.* 1989; Chirone *et al.* 1992; Maring *et al.* 1994, Kruipier *et al.* 1996); the other is by altering the intrinsic properties of particles, e.g. by modifying surface characteristics (Tung, 1981) and mixing with other particles having different sizes or shapes (Wang, 1995).

Numerous applications have been reported for the fluidisation of sub-micron particles such as in the gas-solid hydroxyethylation of potato starch (Kuipers *et al.* 1996) and drying of slurry (Nakagawa *et al.* 1992).

The design and operation of fluidised bed equipment for either chemical or physical processes requires the estimation of the hold up of fines in the bed and the elutriation rate of fines from the bed. On the other hand although many investigators have made extensive investigations on elutriation, nearly all of the existing models or correlations were proposed for Group A and B materials.

This work further investigated the fluidisation behaviour and elutriation phenomena of fine cohesive Group C starch powders from a vibrated fluidised bed column.

EXPERIMENTAL SET-UP AND PROCEDURE

Figure 1 shows the experimental set-up of the vibrating fluidised bed. It consisted of a Perspex cylinder, 150 mm in diameter and 1000 mm length, mounted on top of a vertical vibrating base plate. A filter cloth gas distributor was used to give a pressure drop across the bed of 1 kPa at 4.2 cm/s. A pressure probe connected to a water manometer measured the pressure drop across the bed. A transparent scale was attached on the bed wall to provide direct bed expansion measurement. Air at ambient temperature with a relative humidity of $\pm 50\%$ was used as the fluidising agent. Gas velocities in the range of 0 to 8.8 cm/s were used in this case. Cohesive powders namely glutinous flour, tapioca flour and rice flour were used as feed materials, with properties as listed in Table 1. Bed depth of 20 cm was used in every case.

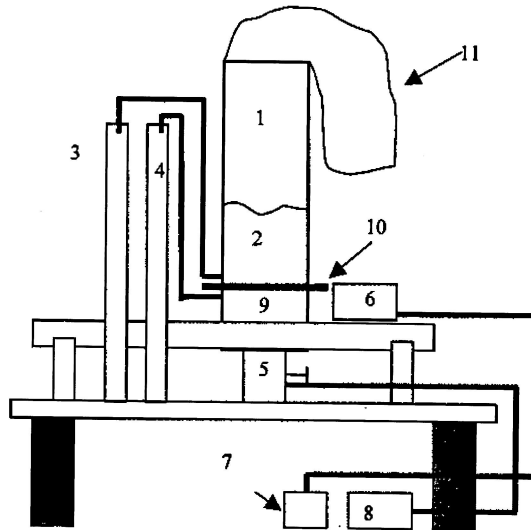


Figure 1. Experimental set-up shows (1) fluidised bed column, (2) the bed, (3) and (4) water manometers, (5) flowmeter, (6) vibrator, (7) inverter, (8) compressor, (9) windbox, (10) distributor, (11) filter bag

Table 1. Properties of base powders

Powder	Mean surface - volume diameter, d_{sv} (μm)	Particle density, ρ_p (kg/m^3)	Moisture content, RH % db.	Hausner ratio, HR (-)
Glutinous flour, GF	34.49	1525	6.39	1.39
Tapioca flour, TF	14.95	1533	6.34	1.37
Rice flour, RF	24.96	1519	6.24	1.38

The strength of vibration is expressed in dimensionless vibration acceleration, Λ , that is the ratio of the vibration acceleration to that of gravity. The index Λ is expressed as follows,

$$\Lambda = A(2\pi f)^2/g \quad (1)$$

where A is amplitude and f is the frequency (50 Hz). Dimensionless vibration acceleration, Λ , in the range of 13 to 18 were used in this study.

Batch entrainment tests were carried out for 10 minutes in every experimental run with gas velocities in the range of 5 to 8.8 cm/s. The total entrainment rates were obtained by weighing

the fines collected in the filterbag. Each series was repeated three times with a new batch of feed material to ensure reproducibility. Size distribution analysis of fines collected was then performed using a Malvern Master Sizer S. Table 2 shows the particle sizes of feed materials referred to as d_{cut} , having a terminal gas velocity, V_t , that equals the operating gas velocities U , and its cumulative percentage in the feed materials. Theoretically, for a given gas velocity, particles equal to and smaller than d_{cut} should be entrained from the bed.

Table 2. Particle size, d_{cut} with V_t equals gas velocity, U , and its % cumulative under in feed materials.

U (cm/s)	Glutinous Flour		Tapioca Flour		Rice Flour	
	d_{cut} (μm)	(%) Cumulative under in feed materials	d_{cut} (μm)	(%) Cumulative in under feed materials	d_{cut} (μm)	(%) Cumulative under in feed materials
5.0	34	51	34	97	34	95
6.6	39	54	39	99	39	96
7.7	41	55	41	100	41	97
8.8	44	56	43	100	44	98

In this case, the elutriation rate constant, K_{ih}^* was calculated from equation (2), as mass of particles in the bed did not change by more than 15%.

$$K_{ih}^* = \frac{M_B}{at} \ln \frac{X_{bit}}{X_{bio}} \quad (2)$$

In equation (2), M_B is mass of solid in bed, a is cross-sectional area of bed, t is elutriation time, X_{bit} is mass fraction of size i in bed after time t , and X_{bio} is mass fraction of size i in bed at $t = 0$.

RESULTS AND DISCUSSION

Fluidisation behaviour of cohesive powder under vibration

Figure 2 shows that pressure drop across the bed increases as vibration increases. A dimensionless index for fluidisation was adopted (Marring *et al.* 1994). The Fluidisation Index, FI , is defined as:

$$FI = \frac{\Delta Pa}{M_B g} \quad (3)$$

where M_B is mass of solid in bed, ΔP is pressure drop across the bed, and g is gravitational acceleration.

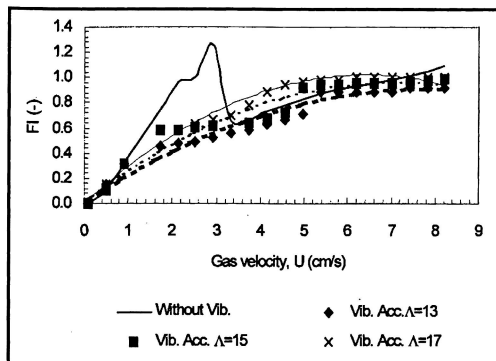


Figure 2a. Glutinous Flour

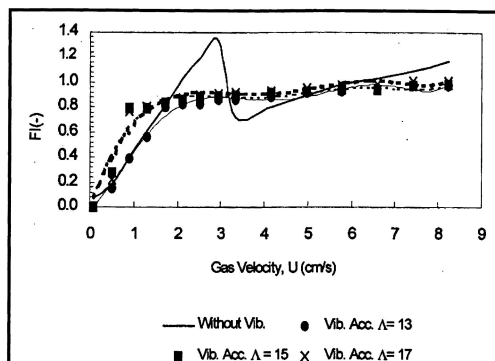


Figure 2b. Rice Flour

Figure 2. Effect of vibration on the pressure drop across the bed for (a) Glutinous flour and (b) Rice Flour

As anticipated, starch powder cannot be fluidised in a conventional way as shown by the abrupt increase of FI for runs without vibration. As has also been reported by other workers (Mori *et al.* 1989; Chirone *et al.* 1992; Maring *et al.* 1994 and Kruipier *et al.* 1996) this was due to the formation of plug and channels in the bed. With vibration, even though FI values were still slightly lower than unity in most cases, it could be observed visually that fluidisation could still be realised. This started with the formation of small horizontal cracks at the bottom of the bed which eventually mutated into bubble like voids, that travelled upwards to the bed surface as the gas velocity increased.

According to visual observation, rice flour fluidised better than tapioca flour in all cases, whilst glutinous flour exhibited poor fluidisation at low gas velocities and gradually improved as a higher gas velocity was supplied. The trend can also be seen from the plots of Fluidisation Index, FI versus gas velocity, U as shown in Figure 3.

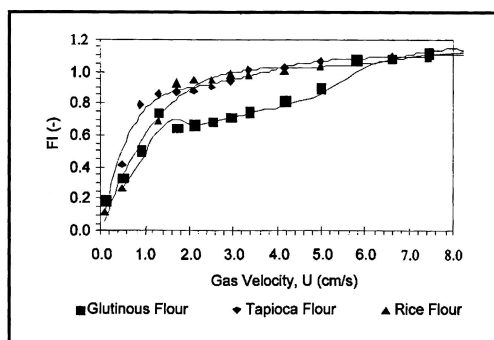


Figure 3a. At dimensionless vibration acceleration, $\Delta = 13$

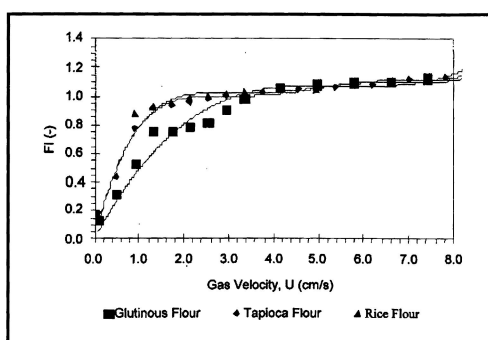


Figure 3b. At dimensionless vibration acceleration, $\Delta = 18$

Figure 3. Plots of FI versus gas velocity, U for different feed materials at (a) $\Delta = 13$ and (b) $\Delta = 18$

Figures 4 and 5 show the effect of vibration on U_{mf} (minimum fluidisation velocity) and ϵ_{mf} (bed voidage at U_{mf}), respectively, obtained for all powders used. U_{mf} in this case was determined from the plot of FI versus gas velocity, whilst ϵ_{mf} was determined from the measurement of bed expansion at U_{mf} . Noda *et al.* (1998) explained the reduction of U_{mf} with the increases of Λ on the basis of void fraction. As has been found from this work, ϵ_{mf} decreases as Λ increases, which explained the reduction of U_{mf} . Similar results have also been reported by Maring *et al.* (1994) when fluidising potato starch in a vibrated fluidised bed.

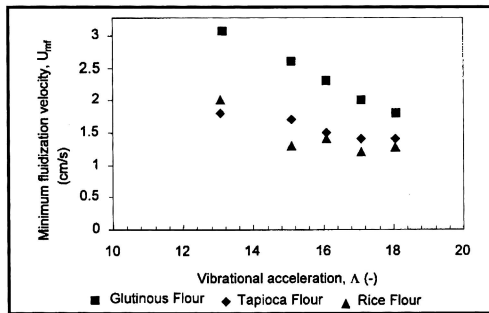


Figure 4. Effect of vibration on minimum fluidisation velocity, U_{mf}

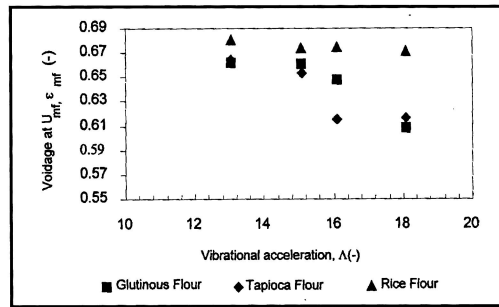


Figure 5. Effect of vibration on voidage, ϵ_{mf}

In this case, when the bed was subjected to vertical vibrations, the shocks from the impacts between bed and distributor caused break-up of particle-particle bonds which are beneficial for fluidisation. As has been shown by Janssen *et al.* (1998), for a given vibration frequency, the relative distributor plate and bed displacement increases as vibration acceleration, Λ , increases. This would bring about bigger forces to break the interparticle bonds to result in better fluidisation and lower U_{mf} compared to vibrations at lower Λ values. The vibration also has the ability to bring particles into close proximity to reduce voidage due to slight compaction when the bed experiences negative displacement or downward movement during one half of the vibration cycle. The equilibrium of these two mechanisms, namely, bed flight to break particle-particle bond and downward movement to induce compaction in the whole vibration cycle will eventually result in stable fluidisation of bed materials.

Janssen *et al.* (1998) and Maring *et al.* (1994) modeled and investigated experimentally the behaviour of aerated, vibrated beds and found the following equation from Carmen-Kozeny for U_{mf} .

$$U_{mf} = \frac{d_{sv}^2 \rho_p g}{180\mu} \frac{\epsilon_{mf}^3}{(1-\epsilon_{mf})} \quad (4)$$

where ϵ_{mf} is bed voidage at U_{mf} , d_{sv} is mean surface-volume diameter of particles, ρ_p is particle density and μ is gas viscosity.

From the values of ϵ_m obtained in this work, comparisons between the experimental values of U_{mf} and values predicted from equation (4) were made. From Figure 6, it can be seen that equation (4) underpredicts the experimental U_{mf} by a certain factor depending on the material used. The finer the particle and hence the more cohesive, the greater the deviation between experimental and predicted U_{mf} .

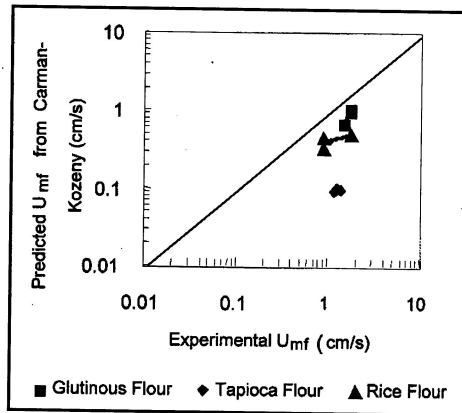


Figure 6. Comparison between experimental and predicted U_{mf}

This may be explained from the fact that particles formed agglomerates in the bed, to give higher U_{mf} than predicted. Figure 7 shows the SEM (Scanning Electron Microscope) images of all feed materials used in the beds. It can be seen that fine particles adhere to each other to form agglomerates with size larger than the actual size of the individual particles. The size of agglomerates, d_{agg} , however could not be determined from these SEM images. Using equation (4), the effective diameter of particles at minimum fluidisation velocity, or mean size of agglomerates d_{agg} , was calculated. Table 3 shows the average values of d_{agg} found for different powders. The d_{agg} values were two or three times larger than the actual mean particle size of each feed material.

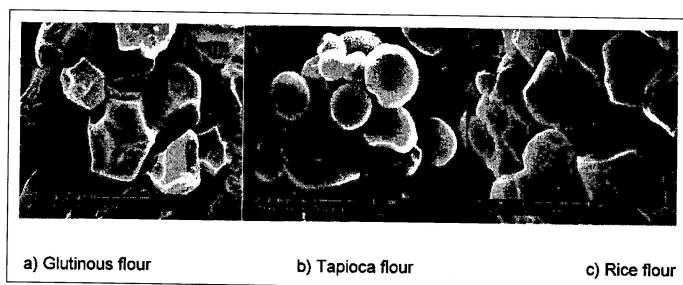


Figure 7. SEM images of materials used in beds.

Table 3. Values of effective mean particle size due to agglomeration in bed, d_{agg} at U_{mf} , calculated from equation (4)

Powder	d_{sv} (μm)	d_{agg} (μm)
Glutinous flour, GF	34.49	65.27
Tapioca flour, TF	14.95	53.32
Rice flour, RF	24.96	45.34

Entrainment flux E_n

Typical example for the effect of vibration on the total entrainment flux, E_n is shown in Figure 8. No obvious trend between the effect of vibration and the total entrainment flux was observed. Figures 9a and 9b show that E_n increases as U increases; and that tapioca flour gave the highest E_n , followed by rice flour and finally glutinous flour. The relationship between E_n and U can be expressed as, $E_n \propto U^n$. Glutinous flour gave the highest dependency value, n , in the range of 1.2 to 2.1; whilst tapioca flour gave a range of 1.2 to 1.6 and rice flour gave 0.9 to 1.4.

It should also be noted that the fraction elutriated from the total fines with size equal to and smaller than d_{cut} is very small, namely in the range of 0.7-1.7 % for glutinous flour, 0.5-0.95 % for rice flour, and 0.7 -1.5 % for tapioca flour. This proves that particles in the bed formed agglomerates with each other to give larger effective size with terminal velocity larger than the operating gas velocity. In this case, elutriation was due to splash of detached fines from agglomerates during ejection of bubbles in the bed surface. The quantity of fines entrained will depend on the initial fines concentration in the bed, hydrodynamic forces acting on the agglomerates as well as the magnitude of adhesive forces between each adjacent particle forming the agglomerates. The magnitude of adhesive forces in this case will depend on factors such as particle size, shape and surface roughness. SEM images suggested that rice flour (Figure 7c) and glutinous flour (Figure 7a) have similar shape and probably surface roughness, which is angular in nature with many smooth flat surfaces to provide areas for contacts. This explains why E_n is lower for rice and glutinous flours than tapioca flour. The shape for tapioca flour (Figure 10) is in most cases spherical in nature with flat surface in certain areas. The higher value of Hausner Ratio (HR) also explains the higher cohesiveness in both glutinous and rice flour (see Table 1).

Elutriation rate constant K_{ih}^*

Plot of the elutriation rate constant, K_{ih}^* , versus gas velocity, U (Figure 10) shows that for all particle sizes K_{ih}^* increases as U increases.

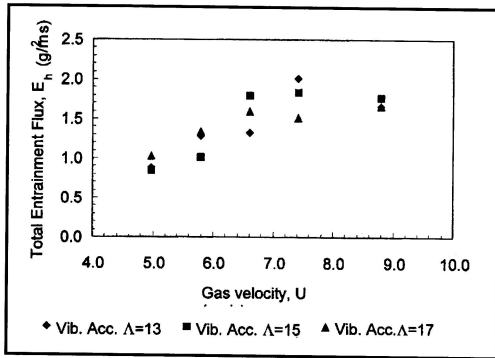


Figure 8a. Rice Flour

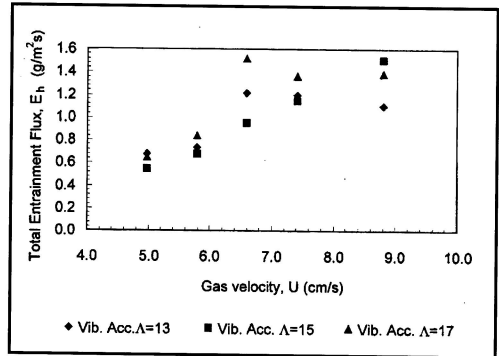


Figure 8b. Glutinous flour

Figure 8. Effect of vibration on total entrainment flux, E_h , for a) Rice flour and b) Glutinous flour

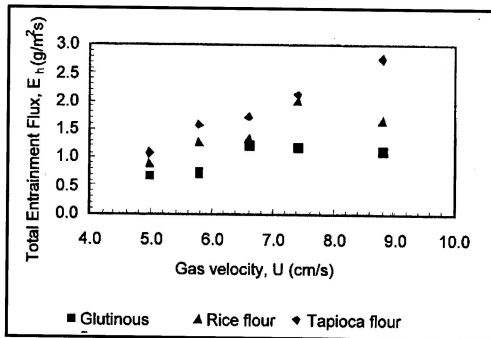


Figure 9a. At vibration acceleration, $\Lambda = 13$

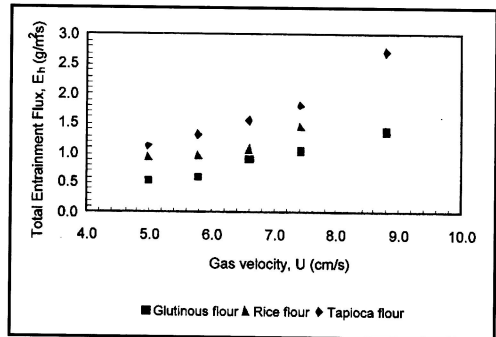


Figure 9b. At vibration acceleration, $\Lambda = 18$

Figure 9. Total entrainment flux, E_h , versus gas velocity, U , for all feed materials vibrated at different vibration accelerations.

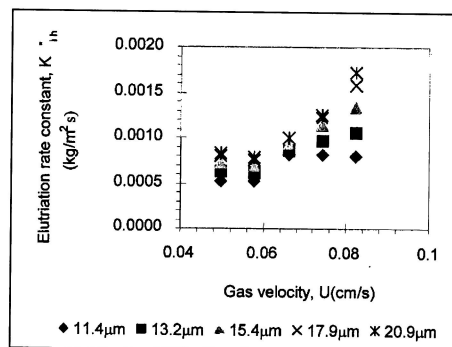


Figure 10. Effect of gas velocity, U , on elutriation rate constant, K_{th} , for different particle size fraction (e.g. glutinous flour)

Figure 11 and Figure 12 show the effect of particle diameter on K_{ih}^* . Baeyens *et al.* (1992), Ma and Kato (1998) and Tasirin and Geldart (1999) found that there exists a certain point at which K_{ih}^* begins to level off or even decreases when using Group A and Group AC powder mixtures. This point is referred to as d_{crit} .

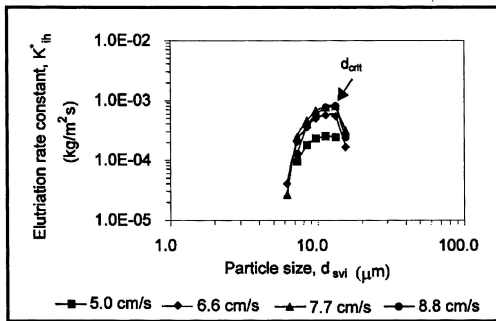


Figure 11. Levelling off of K_{ih}^* for glutinous flour fluidised at different gas velocity, $\Lambda = 15$

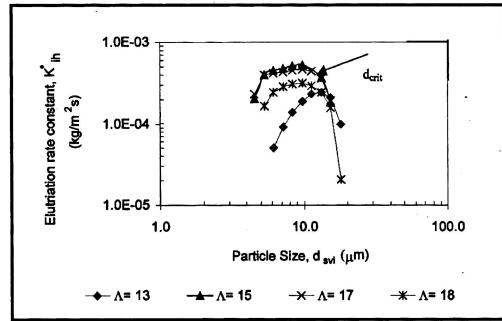


Figure 12. Levelling off of K_{ih}^* for tapioca flour fluidised at different vibration acceleration, $u = 6.6$ cm/s

Baeyens *et al.* (1992) and Ma and Kato (1998) suggested that d_{crit} is the critical particle size at which interparticle forces and gravitational forces are approximately equaled and K_{ih}^* begins to deflect. Baeyens *et al.* (1992) suggested the following equation for the critical size, d_{crit}

$$d_{crit} \rho_p^{0.725} = 10325 \quad (5)$$

where d_{crit} is in micrometers and ρ_p is in kg/m^3

Ma and Kato (1998) suggested equation (6) for the critical size, d_{crit} .

$$\frac{0.455 \rho_p^{0.269}}{\rho_p^d \text{crit} g} = 4.5 \quad (6)$$

Table 4 lists the values of experimental d_{crit} for all feed particles fluidised at different gas velocities, as well as values predicted from equation (5) and equation (6). The experimental values are in all cases smaller than those predicted by the equations. Values calculated from equation (7) as proposed from this work are also listed. Table 5 shows the d_{crit} values at different Λ , for gas velocities of 5 cm/s and 8.2 cm/s.

The effects of gas velocity and vibration on d_{crit} are insignificant, i.e. within $\pm 6.6\%$ deviation in our study; which is in accordance with the findings of other workers (Baeyens *et al.*, 1992 and Ma and Kato, 1998). As suggested by previous workers d_{crit} depends only on the particle density. A value of 4.0 N/m² for the Cohesion Number as suggested by Rietema (1994) was employed to determine the critical cohesion number, N_{coh}^* . In this case, N_{coh}^* was determined as the cohesion number at which the elutriation rates constant, K_{ih}^* is maximum for each

Table 4. Measured and predicted values of d_{crit}

U (cm/s)	Glutinous flour				Tapioca flour				Rice flour			
	Exp*	1*	2*	Equation7	Exp*	1*	2*	Equation7	Exp*	1*	2*	Equation7
5.0	15	51	48	11.2	11.4	51	48	11.1	6.2	53	51	11
6.6	15	51	48	11.2	11.4	51	48	11.1	6.2	53	51	11
7.7	17	51	48	11.2	13.2	51	48	11.1	6.2	53	51	11
8.8	17	51	48	11.2	13.2	51	48	11.1	6.2	53	51	11

Exp*-Experimental values,
 1* - from equation (5) (Baeyens *et al.* 1992),
 2* - from equation (6) (Ma and Kato, 1998).

Table 5. Effect of Λ and U on d_{crit}

$\Lambda(-)$	U = 5 cm/s			U = 8.8 cm/s		
	GF	TF	RF	GF	TF	RF
13	13.2	11.5	8.4	15.2	13.2	7.2
15	13.2	11.4	6.2	15.2	13.2	6.2
16	12.2	13.2	7.2	15.2	13.2	6.2
17	15.0	11.3	7.2	15.2	13.2	6.2

experimental run (Figure 13). It is found that N_{coh}^* differs depending on feed materials used and an average value of 19 was obtained. Using this N_{coh}^* values, equation (6) from Ma and Kato (1998) was modified as equation (7) below;

$$\frac{0.455 \rho_p^{0.269}}{\rho_p^d \text{crit} g} = 19 \quad (7)$$

The values of d_{crit} calculated from equation (7) are shown in Table 4, and found to be in reasonable agreement with the experimental values.

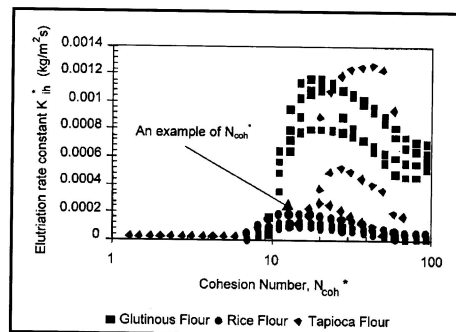


Figure 13. Determination of critical cohesion number, N_{coh}^*

CONCLUSION

It can be concluded that as vibration breaks particle-particle bonds in the bed to induce fluidisation, the formation of agglomerates increases residence time of fines to reduce material loss by entrainment. When starch powders were used as feed materials, entrainment was only in the range of 0.5-1.7 % of the total fines (should be entrained) in the bed. The elutriation rate constants of group C decreases as particle size decreases as reported by other workers. By adapting the criterion proposed by Ma and Kato (1998), it was found in this case that the critical cohesion number, N_{coh}^* is 19.

ACKNOWLEDGEMENT

The authors would like to express their appreciation to UKM and the Government of Malaysia for a grant that makes this study possible. This study was done as part of IRPA 09-02-02-0027 grant.

NOMENCLATURES

A	Amplitude of vibration	(m)
a	Cross-sectional area of bed	(m ²)
d_{cut}	Cut size	(m)
d_{crit}	Critical diameter	(m)
d_{sv}	Surface-volume particle size	(m)
E_h	Total entrainment flux	(kg/m ² s)
f	Frequency	(Hz)
FI	Fluidisation Index	(-)
g	Acceleration of gravity	(m/s ²)
HR	Hausner ratio	(-)
K_{in}^*	Elutriation rate constants	(kg/ m ² s)
M_B	Mass of solid in bed	(kg)
N_{coh}^*	Critical cohesion number	(-)
U	Superficial gas velocity	(m/s)
U_{mf}	Minimum fluidisation velocity	(m/s)
t	Elutriation time	(s)
V_t	Terminal gas velocity	(m/s)
X_{bi}	Size fraction of i in bed after time, t	(-)
X_{bio}	Size fraction size i in bed at $t = 0$	(-)
ϵ_{mf}	Void fraction at U_{mf}	(-)
Λ	Dimensionless vibration acceleration	(-)
ρ_p	Particle density	(kg/m ³)
ΔP	Pressure drop across the bed	(N/m ²)

REFERENCES

- Baeyens, J., Geldart, D. and Wu, S.Y. (1992). Elutriation of fines from gas fluidised beds of Geldart A-type powders - effect of adding superfines, *Powder Technol.*, **71**: pp 71-80
- Chirone, R., L. Massimilla and S. Russo (1992). Bubbling fluidisation of a cohesive powder in acoustic Field, In: *Fluidisation VII*, ed. Potter, O.O and Nicklini, D.J: Engineering Foundation, New York, U.S.A, pp 545
- Geldart, D. (1992). Types of gas fluidisation. *Powder Technol.*, **7**: pp 285-292
- Janssen, L.P.B., Maring, Hoogerbrugge, J.C. and Hoffmann, A.C. (1998). The mechanical behaviour of vibrated, aerated beds of glass and starch powder, *Chem. Eng. Sc.* **53(4)** : pp 761-772
- Kuipers, N.J.M., Stamhuis, E.J. and Beenackers, A.A.C.M. (1996). Fluidisation of potato starch in a stirred vibrating fluidised bed, *Chem. Eng. Sc.*, **51(11)** : pp. 2727-2732
- Ma, X. and Kato, K. (1998). Effect of interparticle adhesion forces on elutriation of fine powders from a fluidised bed of a binary particle mixture, *Powder Technology*, **95** : pp 93 - 101
- Maring, E., Hoffmann, A.C. and Jenssen, L.P.B.M, (1994). The effect of vibration on the fluidisation behaviour of some cohesive powders, *Powder Technology*, **79** : 1-10
- Mori, S, Haruta, T., Yamamoto, A., Yamada, I and Mizutani, E. (1989). Vibro fluidisation of very fine particles, *Kagaku Kogaku Ronbunshu*, **15** : pp 992
- Nakagawa, K, Ohsawa, K., Takarada, T. and Kato, K. (1992). Continuous drying of a fine particles-water surry in a powder-particle fluidised bed, *J. Chem. Eng. Japan*, **25** : pp 495
- Noda, K, Mawatari, K. and Uchida, S. (1998). Flow pattern of fine particles in a vibrated fluidised bed under atmospheric or reduced pressure, *Powder Technology*, **99** : pp 11-14
- Rietema, K. (1984). Powders, What are they ?, *Powder Technology*, **37** : pp 5
- Tasirin, S.M and Geldart, D. (1999). The elutriation of fine and cohesive particles from gas fluidised beds, *Chem. Eng. Comm.*, **173** : pp 175-195
- Tung, Y, (1981). Dynamics of bed collapsing of fluidisation system, M.S. thesis, Institute of Chemical Metallurgy, Academia Sinica
- Wang, Z, L. (1995). Fluidisation of fine particles and the effects of additive particles, Ph.D. thesis, Institute of Chemical Metallurgy, Academia Sinica
- Zhu, Q and Li, H. (1996). Study on magnetic fluidisation of group C powders, *Powder Tech.*, **86** : pp 79